Chapter 7

Frequency-Synthesized Approach to High-Power Attosecond Pulse Generation and Applications: Generation and Diagnostics

Ci-Ling Pan, Hong-Zhe Wang, Rui-Yin Lin, Chan-Shan Yang, Alexey Zaytsev, Wei-Jan Chen and Chao-Kuei Lee

Additional information is available at the end of the chapter

http://dx.doi.org/10.5772/intechopen.78269

Abstract

We present a new scheme of generating high-power attosecond pulses and arbitrary waveform synthesis by multicolor synthesis. The full bandwidth of the multicolor laser system extends more than two-octaves and reaches 37,600 cm^{-1} which can be used to generate sub-single-cycle (~0.37 cycle) sub-femtosecond (360 attosecond) pulses with carrier-envelope phase (CEP) control. The results show a promising approach for generation of relatively high-power attosecond pulses in the optical region. In this chapter, the design and diagnostics of the laser system are described. In part 2 of this work (the following chapter), we demonstrate selected applications of this novel source, such as coherently controlled harmonic generation as well as phase-sensitive 2-color ablation of copper and stainless steel by this multi-color laser system.

Keywords: arbitrary waveform synthesis, harmonic generation, cascaded harmonics, laser ablation, laser sources, pulse generation, multicolored

1. Introduction

Human history has taught us that the invention of novel light sources and related technologies would lead to breakthroughs in science and impact the society and civilization tremendously. X-rays and lasers are good examples of such technologies. High-power laser systems are a class of coherent light sources that play a major role in the advancement of science and

technology, ranging from inertial nuclear fusion, laboratory astrophysics to laser weapons and 3D printing. Such lasers emit continuous wave (CW), nanosecond (ns), picosecond (ps) and femtosecond (fs) pulsed output. Single or near-single cycle electromagnetic radiation can now be generated by laser-based techniques from the terahertz (1 THz = 1012 Hz) to the soft x-ray regions of the spectrum. The spectra of the latter yield attosecond (1 as = 10–18 s) pulses. Such novel sources are expected to have a wide range of potential applications. Attosecond sources [1, 2] are perhaps among the most exciting new laser sources currently under development. In the near future, controlled light wave can steer electrons inside and around atoms. This emerging technology has been dubbed as "lightwave electronics" [3]. Nonetheless, study of condensed matter with attosecond time-resolution remains a challenge [4]. While the potential of microfabrication and nanostructuring of materials by ultrafast lasers were recognized and demonstrated more than a decade ago [5], there have not been reports of real-world applications of attosecond pulses to date. Primarily, this is limited by the lack of powerful attosecond sources.

Among the approaches that allow generation of attosecond pulses, the high-order harmonic generation (HHG) [6] seems to be the most promising one. HHG can serve as a source of intense attosecond pulses that extending from the Vacuum Ultraviolet (VUV) or extreme ultraviolet (EUV) to the soft X-ray region [7]. Alternatively, Chen et al. [8] and Hsieh et al. [9] showed that carrier-envelope-phase (CEP) controlled sub-cycle pulse train can be generated by high-order stimulated Raman scattering (HSRS) process. Recently, we demonstrated the generation of attosecond pulses through pulse synthesis of harmonics of the same laser up to the fifth order. These harmonics were generated through second-order nonlinear optical processes, that is, second harmonic generation (SHG) or sum frequency generation (SFG). This novel source is able to generate sub-single-cycle (~0.37 cycle) pulses with peak intensity of a single pulse as high as 10^{14}W/cm^2, pulse width as short as 400 attosecond with carrier-envelope-phase (CEP) control [10]. Waveform (purple trace) and intensity (red traces) of such ultrashort pulses are shown in **Figure 1**.

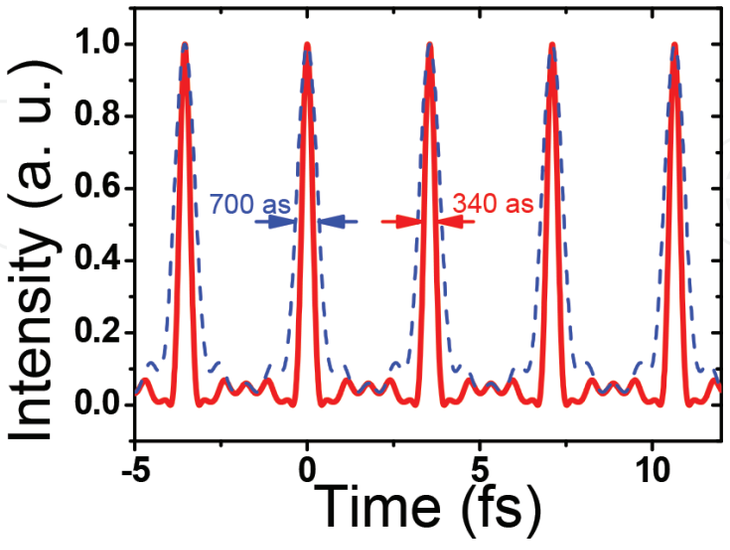

Figure 1. Waveform (blue trace) and intensity (red traces) of sub-femtosecond pulses synthesized by cascaded harmonics of an injection-seed high-power Q-switched laser.

We further show that the relative phase among the optical fields of the harmonics can be maintained a constant at least for thousands of nanosecond pulses. The worst-case relative phase fluctuation is 0.04 π rad. It is shown that sub-femtosecond (360 attosecond) pulses with carrier-envelope phase (CEP) control can be generated in this manner. Synthesis of arbitrary waveforms, for example, square and sawtooth waveforms are possible [11].

Compared to the mainstream method of generating attosecond pulses by higher-harmonic generation (HHG) of few-cycle femtosecond pulses, this novel light source has advantages of compactness and simplicity. Further, arbitrary optical waveform can be synthesized while the attosecond pulse generated in this way is sub-single-cycle with full CEP control. In Section 2 of the chapter, we describe the basic principle for generation of attosecond pulses by synthesis of cascaded harmonics. The prototype system is described. The diagnostics of such broadband sources is nontrivial. Experimental methods for relative phase control among the harmonics are presented in Section 3. This is followed by a review of the synthesis of arbitrary waveforms and their diagnostics by the linear cross-correlation method. Finally, we summarize in Section 5 of the chapter. Applications of this novel high-power laser system can be found in part 2 of this work (the following chapter), in which we discuss coherently controlled harmonic generation [12] as well as phase-sensitive 2-color ablation of copper and stainless steel by this multi-colour laser system.

2. Generation of attosecond pulses by synthesis of cascaded harmonics

Fundamentally, an optical pulse train with a repetition rate of ωm can be viewed as the sum of a set of frequency components that form an arithmetic series [13]. The electric field of each component can be written in the following form:

$$E_q(t) = A_q e^{i\phi_q} e^{i\omega_q t}, \tag{1}$$

where $\omega_q = \omega_0 + q\omega_m$, for $q = 0, 1, 2, \ldots$ To shape the pulse envelope, the phase term ϕ_q and amplitude term A_q of each component are controlled. One can set the phase term ϕ_q and rewrite it as $\phi_q = \phi_0 + q\phi_m$. The synthesized pulse could then be expressed as:

$$E(t) = \sum_q E_q(t) = e^{i(\omega_0 t + \phi_0)} \sum_q A_q e^{iq\omega_m \left(t + \frac{\phi_m}{\omega_m}\right)} = e^{i(\omega_0 t + \phi_0)} E_c\left(t + \phi_m/\omega_m\right), \tag{2}$$

where $E_c(t) \equiv \sum_q A_q e^{iq\omega_m t}$ is a typical cosine pulse train and $\omega_0 t + \phi_0$ is the time-varying CEP with frequency of ω_0. In the commensurate case, the CEP is equal to ϕ_0 for all ultrashort pulses belonging to the same attosecond pulse train or within the ns pulse envelope in the HSRS approach since ω_0 equals to zero. As a result, CEP will be randomly changing if ϕ_0 is random from 1 ns pulse to another. For instance, a 802 nm and a 602 nm laser with pulsewidth around ns and repetition rate of 30 Hz (corresponding to q = 3 and 4 of the Raman resonance of molecular hydrogen) were employed to stimulate the Raman sidebands in early work by one of the co-authors [14, 15]. Because the phases of the two driving lasers, denoted as ϕ_3 and ϕ_4, are random and independent of each other in individual ns pulses, both $\phi_m = \phi_4 - \phi_3$ and

$\phi_0 = \phi_3 - 3\phi_m = 4\phi_3 - 3\phi_4$ are random in time as well. Although CEP of generated pulse trains with 1 ns pulse every 33 ms is fixed. The CEP of attosecond pulses in different ns pulse envelopes varies randomly as well. This severely limits the application of this type of attosecond light source. Cross-correlation by four-wave-mixing interaction among attosecond pulses within the same ns pulse, which are commensurate. Therefore, correlation behavior could still be observed.

Alternatively, CEP will be fixed if all phase-controlled frequency components of the pulse train are optical harmonics from the same laser, rather than through Raman sideband generation. It is clear that the relative phase among generated higher-order harmonics and the lower ones are fixed. For example, relative phase among ϕ_5, ϕ_2 and ϕ_3 of the fifth, second and third harmonic of the same laser will not be changing, if light of frequency ω_5 is generated from SFG of ω_2 and ω_3.

At this junction, it is instructive to note that Hansch proposed that sub-femtosecond pulse could be synthesized by nonlinear phase locking of lasers nearly a decade ago [16]. Later, his group further demonstrated the feasibility of this approach with three cw phase-locked semiconductor lasers [17]. This approach, however, was not pursued since primarily because of the low power generated.

In the following, we summarize the potential advantages and unique features of attosecond pulse generation through pulse synthesis of harmonics of the same laser in contrast to the earlier Raman sideband approach:

2.1. Higher efficiency

This is expected since all the wavelength conversion processes for generation of the harmonics up to the near UV are from second order nonlinearity, instead of third order nonlinearity in the Raman sideband approach.

2.2. Simplicity and compactness

Only one pump laser is required in the present scheme (see **Figure 2(b)**) rather than two in the Raman sideband approach.

2.3. Role of the fundamental frequency

In frequency-domain description of the pulse train, mode spacing or frequency difference of adjacent modes dictates pulse spacing in time or pulse repetition rate in frequency [13]. Therefore, lower-frequency components of the pulse decide the main structure of the pulse waveform while higher-frequency components provide the fine structure or details of the pulse. To illustrate, **Figure 3** shows a square wave synthesized by 10 modes with frequencies from the fundamental to 10th harmonic of the pump laser. Severe distortion is observed if the amplitude of the fundamental is attenuated merely by 10% (see **Figure 3(b)**). This reveals the significance of the component at the fundamental frequency. Significantly, high-quality square

http://dx.doi.org/10.5772/intechopen.78269

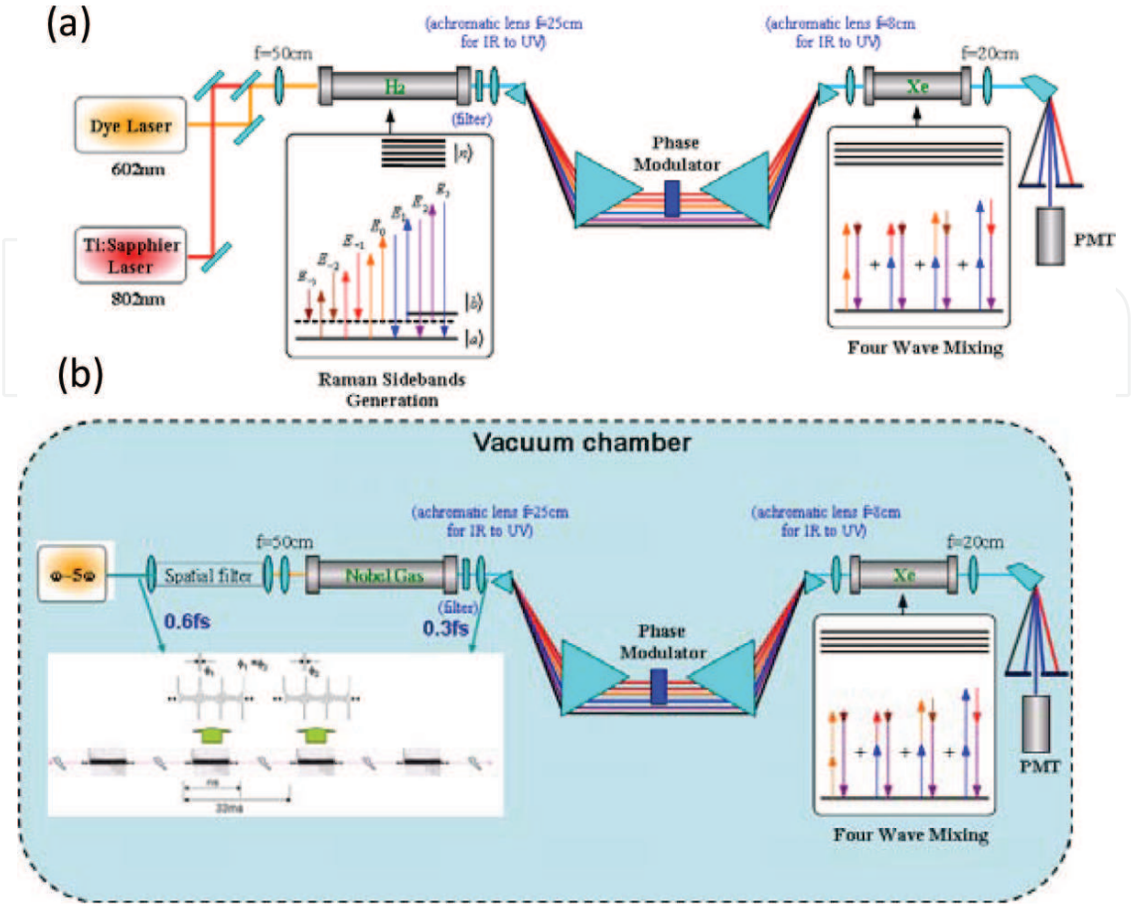

Figure 2. (a) Schematic of the Raman sideband generation approach (b): Schematic of the cascaded harmonics approach A Q-switched Nd:YAG laser and its harmonics up to the fifth order is used as the laser source.

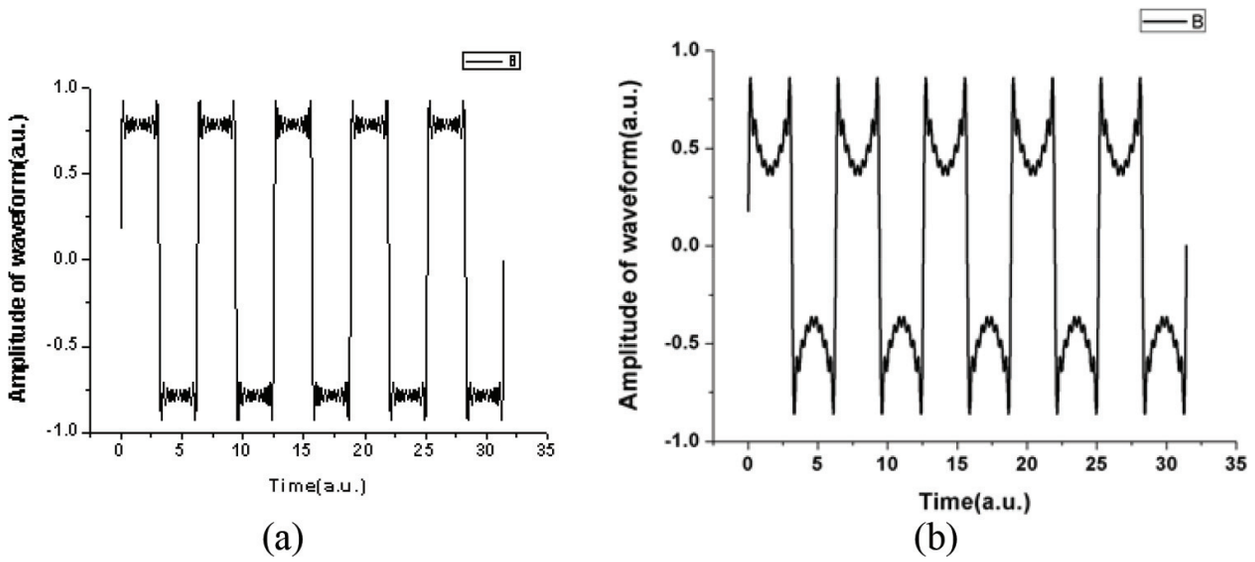

Figure 3. (a) Synthesis of a square wave with modes at frequency from the fundamental to the 10th harmonic of the laser output. (b) Same as (a) except that the amplitude of the mode at the fundamental frequency is attenuated by 10%.

waveform can already be synthesized with five frequency components from the fundamental frequency to fifth harmonic frequency.

2.4. Bandwidth

Compared to the Raman sideband approach, shortest pulse duration generated by the present cascaded harmonics synthesis method is inevitably limited since fewer numbers of channels are available in practice. However, this does not severely limit the application of the latter in generating attosecond pulses. A pulse 0.6 fs in duration could be obtained by synthesis of the fundamental wavelength of 1064 nm and its second, third, fourth and fifth harmonics. This can be understood by realizing that bandwidth is independent of the number of channels physically. These five components already span sufficient bandwidths.

2.5. Pulse quality

Arbitrary waveform synthesis is of importance for attosecond science. As an example, we show the synthesis of a Gaussian pulse with various numbers of frequency components or channels. The image-quality-index, which is widely used in image pattern recognition, is used to gauge the quality of the shaped pulse [18]. The quality increases step-wise only when number of channels is equal to 2^n (n is an integer), that is, 2, 4, 8, 16…). This implies that we do not have to put too much effort into generating the sixth and seventh harmonic unless the 8th harmonic (133 nm) can be generated efficiently as well (**Figure 4**).

As a further example, we show the synthesis of a sawtooth waveform with various numbers of channels (see **Figure 5(a)**). **Figure 5(a)** also indicates that a quality factor of 92% could be achieved already with 4 channels. The perfect sawtooth wave, those synthesized with 4 channels (from the fundamental to the fourth harmonics) and 32 channels (from the fundamental to the 32nd harmonics) are illustrated in **Figure 5(b)**. The sawtooth waveform synthesized with 4 channels is already recognizable, while that generated with 32 channels is indistinguishable from the mathematical function.

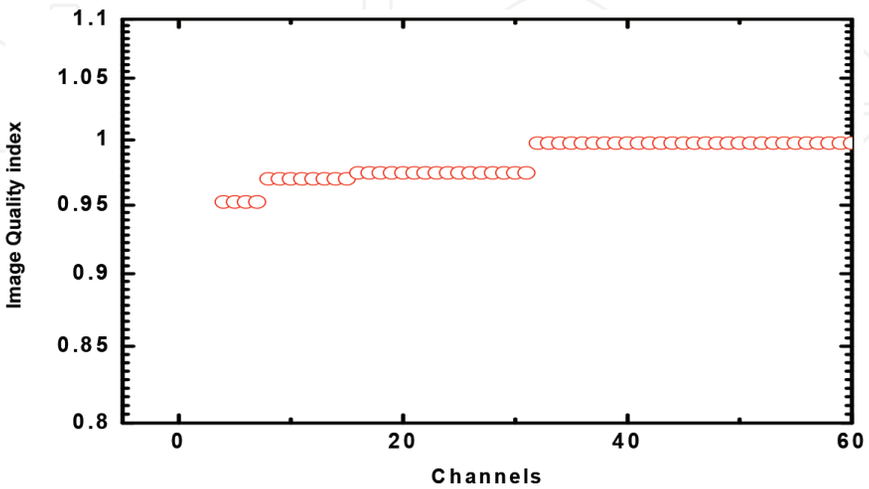

Figure 4. Image quality index of a Gaussian pulse generated with different number of channels.

http://dx.doi.org/10.5772/intechopen.78269

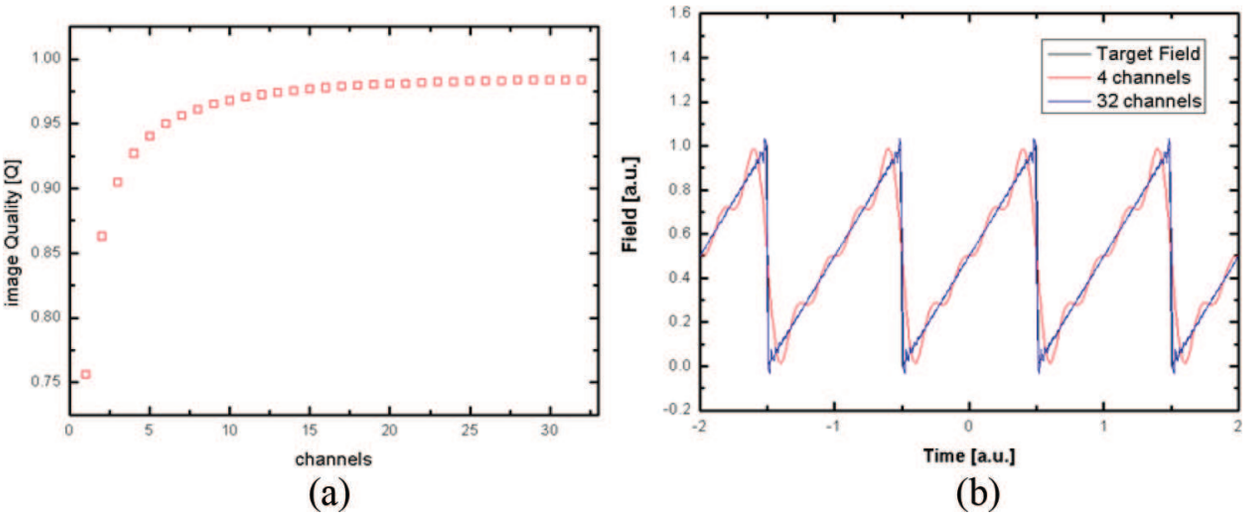

Figure 5. (a) Synthesis of a sawtooth waveform with various numbers of channels (b) the perfect sawtooth wave, those synthesized with 4 channels (from the fundamental to the fourth harmonics) and 32 channels (from the fundamental to the 32th harmonics).

In our lab, we have constructed a system for the demonstration of attosecond pulse generation by synthesis of cascaded harmonics. This is shown in **Figure 6**. The fundamental frequency component at ω_1 is from a custom-made injection-seeded Quanta Ray PRO- 290 Q-switched Nd:YAG laser (λ = 1064 nm) operating at 10 Hz. The pulse duration is about 10 ns. The laser frequency bandwidth is narrower than 0.003 cm^{-1}. The nonlinear optical crystals for generating 2nd through the 5th harmonics of the laser fundamental beam are arranged in a cascaded layout. The crystals are KD*P type II for the second harmonic ω_2, KD*P type I for the third harmonic ω_3, BaB_2O_4 (BBO) type I for the fourth harmonic ω_4, and BBO type I for the fifth harmonic ω_5. Thus the five-color output of the laser system covers optical spectra from the near infrared (NIR) or 1064 nm to the ultraviolet (UV), that is, 213 nm. The cascade setup was adopted to ensure that the second-order nonlinear optical process all occurred collinearly. As a result, the fundamental and harmonics overlapped spatially. The pulse energy of each harmonic was 380, 178, 70, 41, and 22 mJ, respectively. The polarizations of the five colors were elliptic, horizontal, vertical, vertical, and horizontal for the fundamental through the fifth harmonic in that order. Eventually, all five colors will be converted into horizontally polarized light (see below).

Precision control of the amplitude and the phase of each frequency components are essential. To this end, we first spatially dispersed the five colors by a fused silica prism. The dispersed beams were then recollimated but spatially separated by using another, larger fused silica prism. In the parallel co-propagating region of the five colors, we inserted an amplitude modulator and a phase modulator each. Therefore, it is possible to adjust the amplitude and relative phase of these harmonics separately. Each amplitude modulator was the assembly of a half waveplate and a polarizer. The polarization directions of the harmonic frequencies were all horizontal after passing through the polarizers. We can adjust the pulse energy of each harmonic by rotating the orientation of the half waveplate. To deal with the elliptical polarization of the fundamental frequency of the laser, we used a quarter waveplate to rotate the elliptical polarization back to the linear polarization.

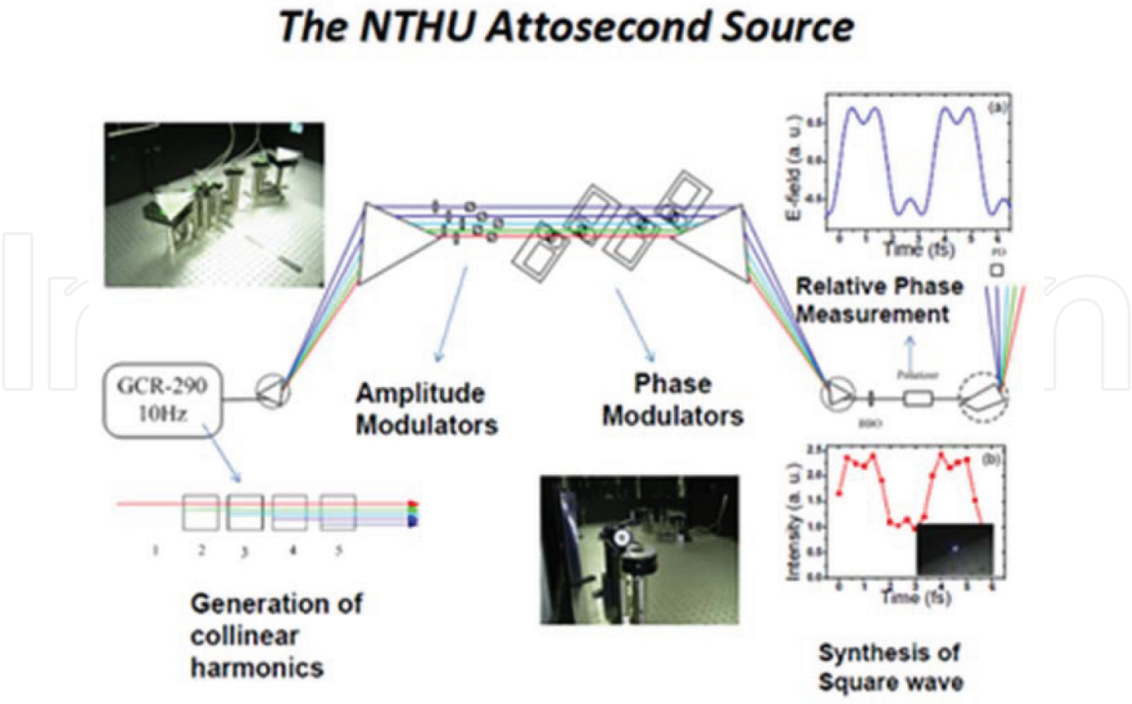

Figure 6. First-generation NTHU Attosecond source based on frequency synthesis of cascaded in-line harmonics of a single-frequency Q-switched Nd:YAG laser. Amplitude and phase modulation of each of the harmonics are provided. Insets (a) and (b) show predicted and experimentally generated square waveforms.

Each phase modulator consisted of a pair of right-angle triangle prisms. Adjusting the relative positions of each prism in the pair independently along the direction of their hypotenuse will change the effective path length traveled by each harmonic. The phase of each harmonic wave will be altered by $\Delta\phi_i = 2\pi\ (n_{prism} - n_{air})l/\lambda_i$, where l is the relative displacement of the two prisms n_{prism}, and n_{air} are refractive indices of the prism and air, respectively. This scheme allows variation of the phase $\Delta\phi_{\text{i}}$ of the i_{th} harmonic, i = 1–5, but will not affect the beam alignment. Finally, these five beams of fundamental output and cascaded harmonics of the Nd:YAG laser were recombined and collimated by another prism set at a symmetry position to the first prism set. The whole setup is similar to a 4-f imaging system.

3. Relative phase measurement

For waveform control and pulse synthesis, we need to determine the relative phase among the harmonics. This was accomplished as follows: First, the fifth harmonic was used as the reference. We then proceed to adjust the relative phase of all other four harmonic frequencies to the reference. Four type I BBO crystals were employed. These were cut at (a) $\theta = 22.9°$ and $\phi = 0°$ for 1064 nm + 1064 nm → 532 nm, (b) $\theta = 31.3°$ and $\phi = 0°$ for 1064 nm + 532 nm → 355 nm, (c) $\theta = 47.7°$ and $\phi = 0°$ for 532 nm + 532 nm → 266 nm, and (d) $\theta = 51.2°$ and $\phi = 0°$ for 1064 nm + 266 nm → 213 nm, respectively. The Nd:YAG laser harmonic frequencies and summed frequencies generated from the BBO crystal were then dispersed and detected by a

set of photodiodes. Every harmonic was heterodyned with a signal at the same frequency derived by optically summing two lower harmonics in a particular BBO crystal. Then the resulting interference signal can be used to calibrate the phase modulator and to align the phases of the harmonic frequencies. Since the polarization of the summed output is orthogonal to that of the harmonics, a polarizer is used to project the polarization of the two states onto a common axis in order to maximize the heterodyning signal. With five frequency components, four measurements are needed for determining of their relative phases. The setup of the relative phase between each harmonic is shown as **Figure 7**.

The flow chart of determining the relative phase of the second harmonic (532 nm) with respect to the fundamental by measuring the interference signal is shown in **Figure 8**. First, light from the laser system at ω_1 and ω_2 generates the signal at ω_3' through the sum-frequency generation (SFG) in a BBO crystal. By tuning the phase modulator inserted in the beam path of the light at ω_3 from the laser signal, we can introduce a phase difference $\Delta\phi_3$ between the harmonic from the laser system and light of the same frequency from the sum-frequency generation process. For the case of 355 nm light (see **Figure 9**),

$$\Delta\phi_{355} = \phi'_{355} - \phi_{355} = \phi_{1064} + \phi_{532} + \frac{\pi}{2} - \phi_{355}$$

Or

$$\phi_{355} = 3\phi_{1064} + \pi - \Delta\phi_{532} - \Delta\phi_{355} \tag{3}$$

As the phase modulator is tuned, the interference signal shows the expected sinusoidal behavior (see **Figure 9**). After the relative phase changes over a few cycles, the scan is stopped (middle of **Figure 9**). This part of the interference record reflects the phase stability of the system, as the phase and power of the harmonics do vary in practice.

The phase stability of the third-harmonic beam at 355 nm is 0.0407 π, while that of the second harmonic is 0.1103 π. It is possible to control the phase modulator such that the interference

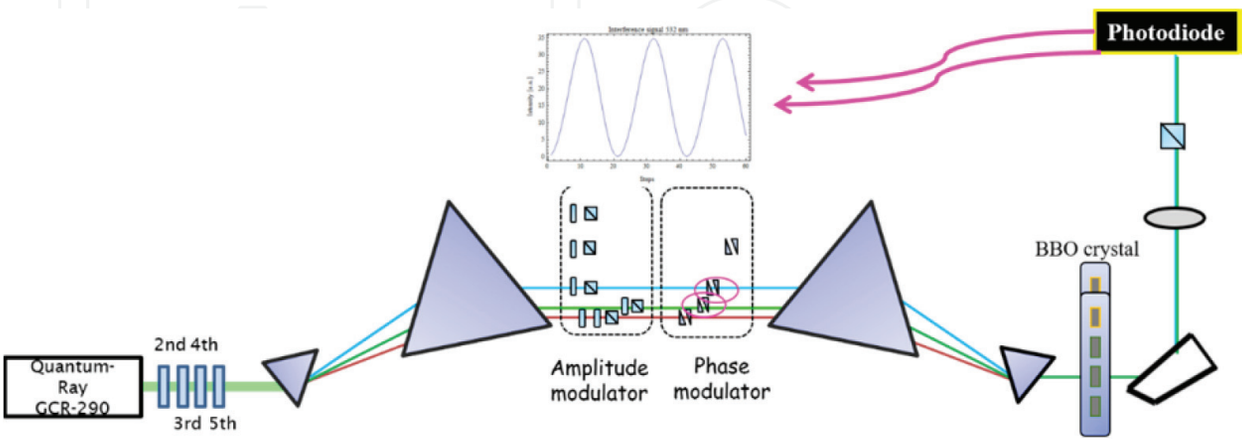

Figure 7. The experimental setup for relative phase measurement. Four BBO crystals were used. Second, third, fourth and fifth indicate the nonlinear crystals in the cascaded generation process.

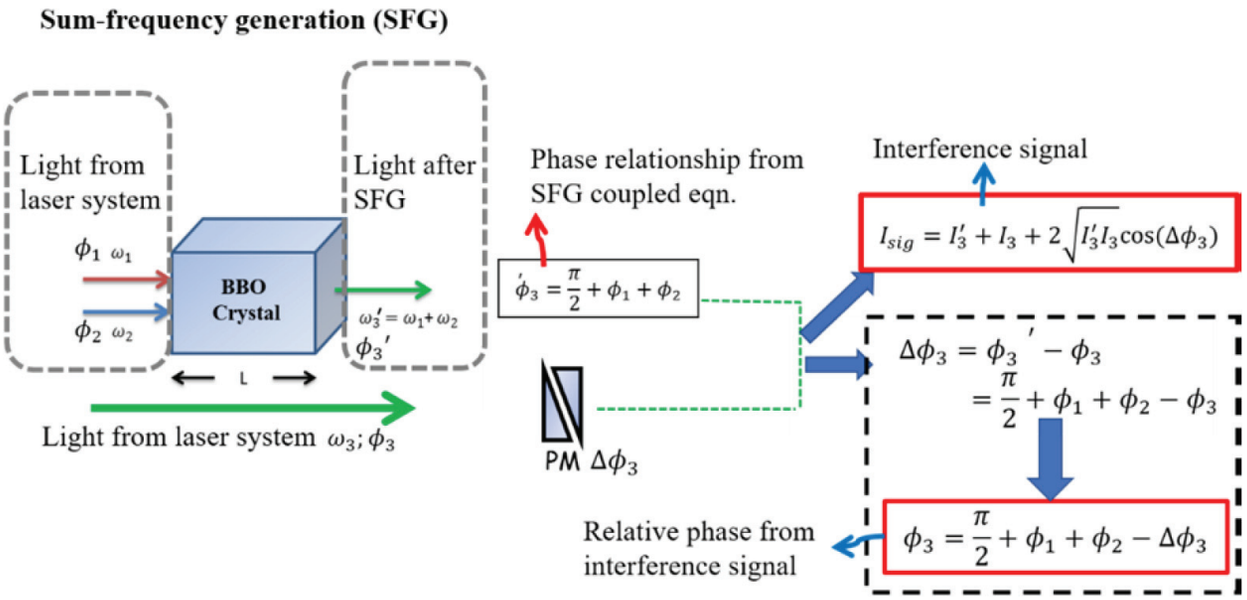

Figure 8. The flow chart for measuring the relative phase through the interference signal.

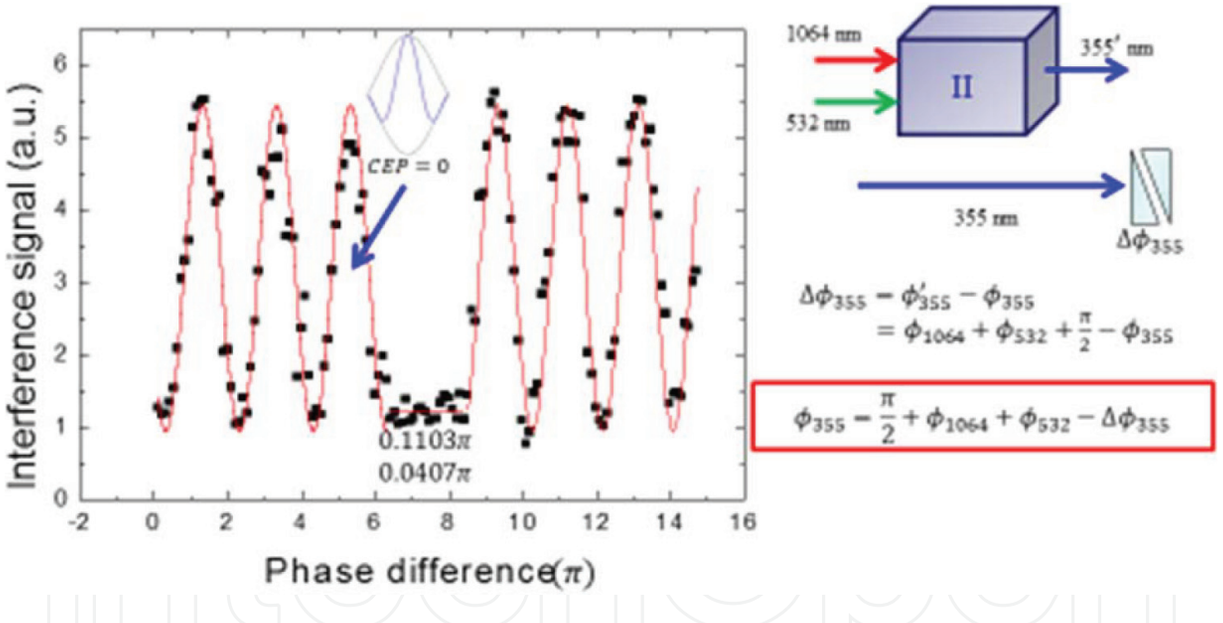

Figure 9. The relative phase between fundamental and the third harmonic is determined as shown on the right of the figure. Left of the signal shows the experimentally measured interference signal. CEP: carrier envelope phase.

signal is maintained at certain level, for example, the half, the maximum, and the minimum of the magnitude of the interference signal. For example, we fixed $\Delta\phi_{532} = \pi/2$. When the interference signal at 355 nm is at half of the maximum intensity, the phase difference $\Delta\phi_{355}$ is 0.5π. According to Eq. (3), the relative phase relationship is $\phi_{355} = 3\phi_{1064}$ which is the phase-matching condition. The carrier envelope phase of the synthesized wave or CEP is zero. Similarly, if we set the phase difference $\Delta\phi_{355}$ to be 0. $\phi_{355} = 3\phi_{1064} + \pi/2$. Therefore, the CEP of the synthesized waveform is $\pi/2$.

4. Waveform synthesis and its measurement

As the spectral bandwidth of this coherent laser source exceeds two octaves or 32,200 cm^{-1}, conventional methods for ultrafast waveform synthesis is not adequate. We used the shaper-assisted linear correlation method [19] for such a task. This method is particularly suited for diagnostics of multiwave synthesized waveforms.

The basic concept is the use of an effective delta function waveform to retrieve the waveform. To begin with, the output electric field of a coherent multiwave synthesized optical waveform, for example, a mode-locked laser can be expressed as:

$$E_a(t) = \sum_{n=1}^{N} a_n \cos\left(n\omega t + \phi_{an\omega} + \phi_{aCEP}\right) \tag{4}$$

where a_n *and* $\phi_{an\omega}$ are the amplitude and phase of each component at the frequency $n\omega$, n is a positive integer. ϕ_{aCEP} is the carrier envelope phase. Considering two such waveforms, one is the reference with field $E_a(t)$ above and the target waveform with field $E_b(t)$, given by

$$E_b(t) = \sum_{n=1}^{N} b_n \cos\left(n\omega t + \phi_{bn\omega} + \phi_{bCEP}\right). \tag{5}$$

The interference of the two with a relative temporal delay τcan be described as follows:

$$E_T(t,\tau) = \frac{1}{2}\sum A_n e^{i\left(n\omega t + \phi_{n\omega}\right)} + c.c. \tag{6}$$

$$(\text{where})\ A_n = \sqrt{a_{n+}^2 b_n^2 + 2a_n b_n \cos\left(n\omega\tau + \left(\phi_{bn\omega} - \phi_{an\omega}\right) + \phi_{bCEP} - \phi_{aCEP}\right)}$$

$$\phi_n = \cos^{-1}\left[\left(\left(a_n \cos\left(\phi_{an\omega} + \phi_{aCEP}\right) + b_n \cos\left(n\omega\tau + \phi_{bn\omega} + \phi_{bCEP}\right)\right)/A_n\right]\right.$$

A_n *and* $\phi_{n\omega}$ are the amplitude and phase of the n_{th} Fourier component of the interference signal. The linear cross-correlation function of the reference and target signals with a relative time delay of τ. The time-averaged intensity of E_T is then given by

$$\begin{aligned} \mathrm{I}(\tau) &= \frac{1}{T}\int E_T(t,\tau)E_T^*(t,\tau)dt = \frac{1}{4}\sum_n A_n^2 \\ &= \sum\left(a_{n+}^2 b_n^2 + 2a_n b_n \cos\left(n\omega\tau + n\left(\phi_{bn\omega} - \phi_{an\omega}\right) + \phi_{bCEP} - \phi_{aCEP}\right)\right) \end{aligned} \tag{7}$$

If the reference waveform is a transform-limited cosine pulse function of finite duration or a delta function of unity amplitude, that is, $a_n = a_0$, phase $\phi_{an\omega} = 0$, $\phi_{aCEP} = 0$

$$\mathrm{I}(\tau) = \sum\left(a_{0+}^2 b_n^2\right) + 2a_0 b_n \cos\left(n\omega\tau + \phi_{bn\omega} + \phi_{bCEP}\right) \tag{8}$$

That is, the time-varying part of I(τ) is directly proportional to the target field, Eb(t) (see Eq. (6)). If the reference pulse and target one are delta and square pulse, Eq. (5) can be written as

$$\begin{aligned} E(t,\tau) &= E_\delta(t) + E_{square}(t,\tau) \\ &= A_\delta \sum_n e^{i(\omega_n t - k_n d)} + B_{squ} \sum_{n=1,3,5,..} \frac{2}{n\pi} e^{i\left(\omega_n(t-\tau) - k_n d - \frac{\pi}{2}\right)} \\ &= \sum_n \mathrm{e}^{i\omega_n t} A_n'(\tau) e^{i\varphi_n'(\tau)} \end{aligned} \tag{9}$$

where

$$A_n' = \sqrt{{A_\delta}^2 + \left(\frac{B_{squ}}{n}\right)^2 + 2A_\delta \frac{B_{squ}}{n} \cos\left(\omega_n \tau - \frac{\pi}{2}\right)},$$

$$\varphi_n' = \tan^{-1}\left[\frac{-A_\delta \sin(k_n d) + \frac{B_{squ}}{n}\sin\left(\omega_n \tau - \frac{\pi}{2} - k_n d\right)}{A_\delta \cos(k_n d) + \frac{B_{squ}}{n}\cos\left(\omega_n \tau - \frac{\pi}{2} - k_n d\right)}\right] \quad \text{for n} = 1, 3, 5.. \tag{10}$$

$$A_n' = A_\delta, \quad \varphi_n' = -k_n d \qquad \text{for n} = 2, 4, 6.... \tag{11}$$

The linear cross-correlation measurement can be performed using any interferometric arrangement, for example, a Michelson interferometer. Equivalently, it can be conducted by adjusting the amplitudes and phases of the frequency components of the waveform. The experimental setup is shown in **Figure 10**. A thermal pile power meter, which can detect light from the fundamental (λ = 1064 nm) to the fifth harmonic (λ = 213 nm) of the laser system.

We have shown previously that it is possible to synthesize attosecond pulse train and arbitrary waveforms using this approach [11]. For example, **Figure 11(a)** shows the synthesized square waveform by the fundamental, second and third harmonics of the Nd:YAG laser. The normalized amplitudes of the harmonics are respectively, 1, 0 and 1/3. **Figure 11(b)** shows the synthesized sawtooth waveform by the fundamental through the fourth harmonics of the Nd:YAG laser. The normalized amplitudes of the fundamental and harmonics are respectively, 1, 1/2, 1/3 and 1/4. The measured waveforms are in good agreement with the theoretical estimates (solid curves in **Figure 11**). Although we just used three of four waves in this experiment, the synthesized waveforms already reproduce these familiar mathematical functions.

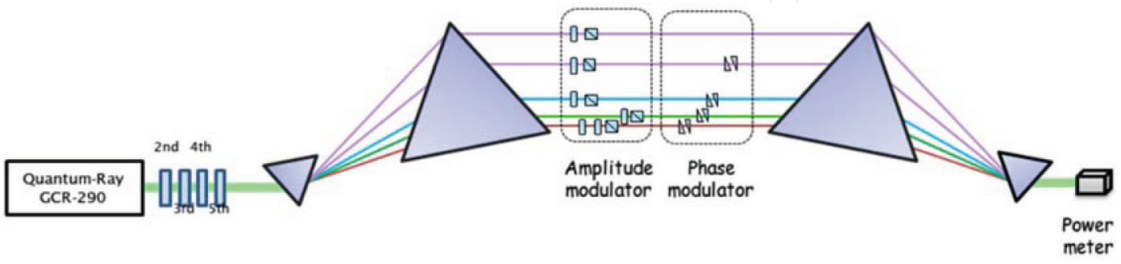

Figure 10. The experimental arrangement for linear cross-correlation measurement of the synthesized waveform. Second, third, fourth and fifth indicate the nonlinear crystals that generated the cascaded harmonics.

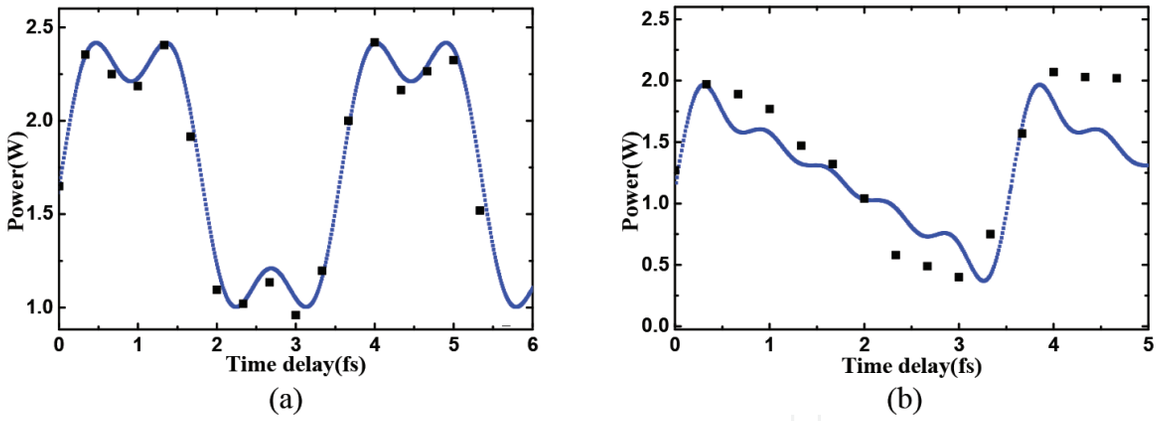

Figure 11. (a) Synthesis of a square waveform with the fundamental, second and third harmonics of the Nd:YAG laser. (b) Synthesis of a sawtooth waveform with the fundamental, second, third and fourth harmonics of the Nd:YAG laser. The solid squares are experimental data. The blue curves are theoretical curves. (reproduced with permission from [11]).

Our laser system can generate fundamental through the fifth harmonics with pulse energies of 380, 178, 70, 41, and 22 mJ. If these can be fully utilized, the synthesized transform-limited pulse will exhibit a temporal FWHM of 480 attoseconds. The intensity envelope will be just 700 attoseconds. The intensity of each attosecond pulse will exceed 10^{14} W/cm^2 when it is focused to a spot size of 20 μm. Such high-power pulses would induce interesting nonlinear effect in materials. Opportunities in novel laser processing should arise. These will be discussed in the part II of this work.

5. Summary

We proposed and demonstrated a new high-power attosecond light source by frequency synthesis. The laser system consists of a narrow-band transform-limited high-power Q-switched Nd:YAG laser and its second (λ = 532 nm) through fifth harmonics, (λ = 213 nm). The laser system was designed such that the cascaded harmonics spatially overlap and co-propagate to the far fields. The spectral bandwidth of this coherent laser source thus exceeds two octaves or 32,200 cm^{-1}.The amplitude and phase of the comb consisting of the five frequency components can be independently controlled. Sub-single-cycle ($\sim$ 0.37 cycle) sub-femtosecond (360 attosecond) pulses with carrier-envelope phase (CEP) control can be generated in this manner. The peak intensity of each pulse exceeds 10^{14} W/cm^2 with a focused spot size of 20 μm. It is also possible to synthesize arbitrary optical waveforms, for example, a square wave. The synthesized waveform is stable at least for thousands of nanosecond.

Acknowledgements

This work was supported by grants sponsored by the National Science Council of Taiwan (NSC 98-2112-M-009-015-MY3) and Phase II of the Academic Top University Program of the Ministry of Education, Taiwan.

Author details

Ci-Ling Pan[1]*, Hong-Zhe Wang[1], Rui-Yin Lin[2], Chan-Shan Yang[3], Alexey Zaytsev[1], Wei-Jan Chen[1] and Chao-Kuei Lee[4]

*Address all correspondence to: clpan@phys.nthu.edu.tw

1 Department of Physics, National Tsing Hua University, Hsinchu, Taiwan

2 Department of Photonics, National Chiao Tung University, Hsinchu, Taiwan

3 Institute of Electro-Optical Science and Technology, National Taiwan Normal University, Taipei, Taiwan

4 Department of Photonics, National Sun Yat-Sen University, Kaoshiung, Taiwan

References

[1] Helmer M. Nature Milestones: Photons, Milestone. Attosecond science 1 May, 2010;Vol. 22; 2001. doi:10.1038/nmat2659

[2] Krausz F, Ivanov M. Reviews of Modern Physics. 2009;**81**:163

[3] Goulielmakis E, Yakovlev VS, Cavalieri AL, Uiberacker M, Pervak V, Apolonski A, Kienberger R, Kleineberg U, Krausz F. Science. 2007;**317**:769-775

[4] Cavalieri AL, Müller N, Uphues T, Yakovlev VS, Baltus caronka1 A, Horvath B, Schmidt B, Blümel L, Holzwarth R, Hendel S, Drescher M, Kleineberg U, Echenique PM, Kienberger R, Krausz F, Heinzmann U. Nature. 2007;**449**:1029-1032

[5] Liu X, Du D, Mourou G. IEEE Journal of Quantum Electronics. 1997;**33**:1706-1716

[6] Lewenstein M, Balcou P, Ivanov MY, L'Huillier A, Corkum PB. Physical Review A. 1994; **49**(3):2117-2131

[7] Midorikawa K, Nabekawa Y, Suda A. XUV multiphoton processes with intense high-order harmonics. Progress in Quantum Electronics. 2008;**32**(2):43-88

[8] Chen W-J, Hsieh Z-M, Huang SW, Su H-Y, Lai C-J, Tang T-T, Lin C-H, Lee C-K, Pan R-P, Pan C-L, Kung AH. Physical Review Letters. 2008;**100**:163906

[9] Hsieh Z-M, Lai C-J, Chan H-S, Sih-Ying W, Lee C-K, Chen W-J, Pan C-L, Yee F-G, Kung AH. Physical Review Letters. 2009;**102**:213902

[10] Chen W-J, Lee C-K, Pan C-L. Paper FWE6, Presented at the Frontiers in Optics 2010/Laser Science XXVI, OSA Technical Digest (CD); Rochester, New York, USA; Oct. 2010. pp. 24-28

[11] Chen W-J, Wang H-Z, Lin R-Y, Lee C-K, Pan C-L. Laser Physics Letters. 2012;**9**(3):212

[12] Chen W-J, Lin R-Y, Chen W-F, Lee C-K, Pan C-L. Laser Physics Letters. 2013;**10**:065401

[13] Goodman JW. Introduction to Fourier Optics. New York: McGraw-Hill; 2002

[14] Chen W-J, Kung AH. Optics Letters. 2005;**30**:2608

[15] Huang SW, Chen WJ, Kung AH. Physical Review A. 2006;**74**:063825

[16] Hansch TW. Optics Communications. 1990;**80**:71-75

[17] Mukai T, Wynands R, Hansch TW. Optics Communications. 1993;**95**:71-76

[18] Wang Z, Bovik AC. IEEE Signal Processing Letters. 2002;**9**:81-84

[19] Chan H-S, Hsieh Z-M, Liang W-H, Kung AH, Lee C-K, Lai C-J, Pan R-P, Peng L-H. Science. 2011;**331**:1165-1168

IntechOpen